Fractal Growth Phenomena

Tamás Vicsek

Institute for Technical Physics
Budapest, Hungary

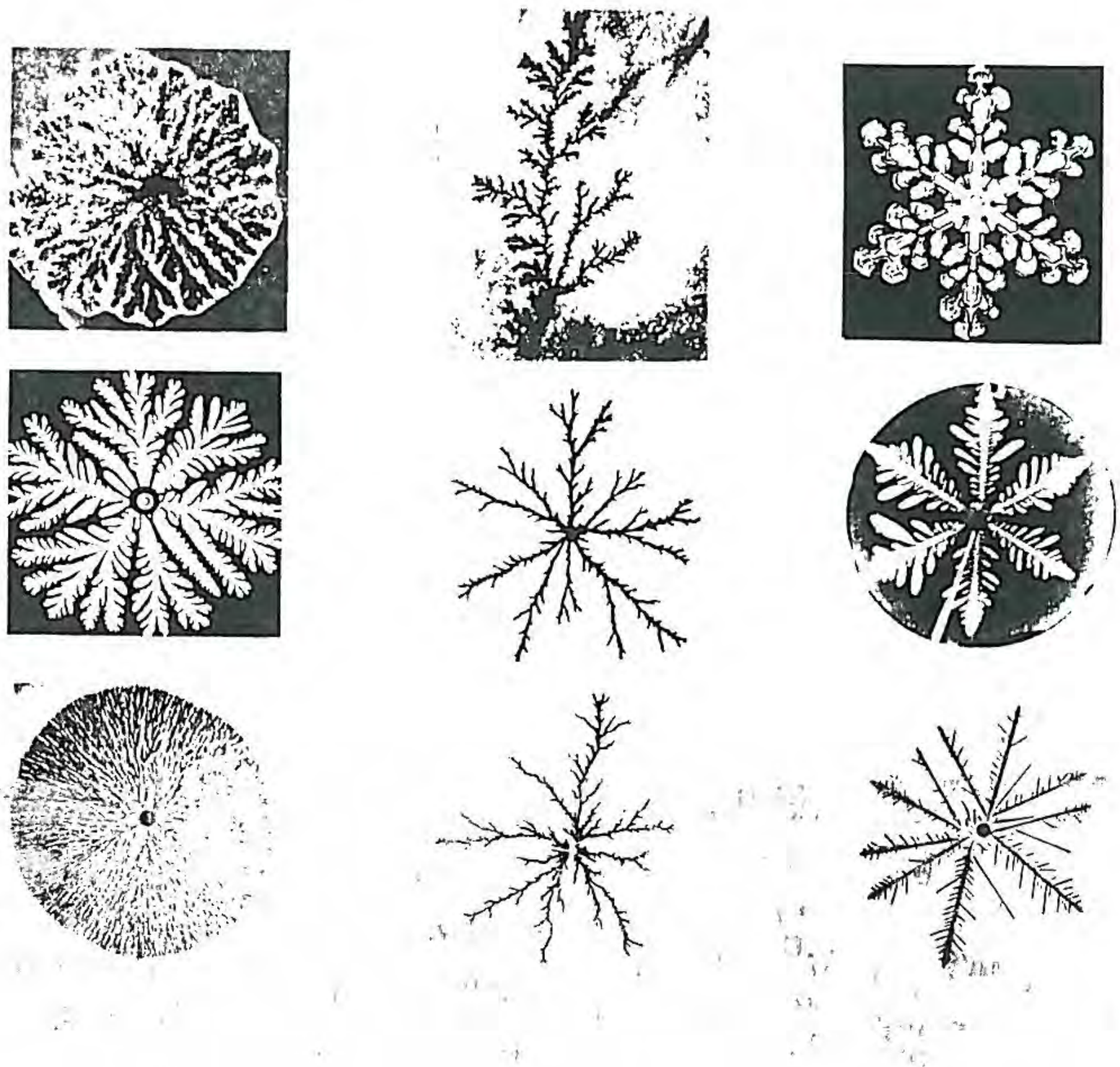

WORLD SCIENTIFIC
Singapore

$D = A \cdot b^{\alpha}$

/

Scaling, $C(r) \sim A r^{\alpha}$ $r \to br$ $C(br) \sim D r^{\alpha}$
new - analitikus, kritikus viselkedés, kritikus pont
universális kritikus exponenser

PART II.

CLUSTER GROWTH MODELS

Chapter 7.

GROWING SELF-AFFINE SURFACES

Many growth processes lead to space filling objects with a trivial dimension coinciding with the dimension of the space d in which the growth takes place. However, the surface of these objects may exhibit special scaling behaviour. The three basic possibilities are the following: the surface may be i) smooth, having a trivial dimension $d_s = d - 1$, ii) fractal with $D < d$ and iii) self-affine, characterized by an anisotropic scaling of the typical sizes. In this chapter cluster growth models producing the third kind of interfaces will be discussed.

Irreversible growth phenomena rarely result in smooth surfaces. Determining the fractal dimension of a self-similar interface is an important step in characterizing its properties. There are a number of known examples for such surfaces, including shore lines and the surface of silica colloid particles or materials used for catalysis. *Self-similarity*, however, implies the presence of "*overhangs*" in the surface structure: to satisfy isotropic scale invariance all possible directions should be represented equally.

During the growth of compact (non-fractal) objects the motion of the interface is directed outward, and this orientation plays a special role. Typically, the interface can be well approximated by a *single valued* function

of $d-1$ variables, e.g., one can describe the properties of the surface by examining only those points of the object which are the farthest from the centre of the structure in a given direction. The scaling properties of such surfaces (with irrelevant overhangs) are *direction dependent*: parts of various sizes can be rescaled into an object with the same overall behaviour using a rescaling factor in the direction parallel to the growth which is different from that needed to rescale the perpendicular lengths.

Mathematical examples for self-affine surfaces invariant under anisotropic rescaling of distances were discussed in Section 2.3.2. It was shown that for these objects there exists a crossover scale x_c separating two regimes. For example, the local fractal dimension of a self-affine fractal embedded in two dimensions can be observed only for length scales $x \ll x_c$, while for sizes $x \gg x_c$ the object has a global fractal dimension $d = 1$. It is important to realize that for cluster growth models $x_c = a$, where a is the lattice constant. Since a cluster of particles of size a does not have any detail on a length scale smaller than a, we conclude that *no local fractal dimension* can be associated with growing self-affine surfaces generated on a lattice.

7.1. EDEN MODEL

Perhaps the simplest cluster growth model was introduced by Eden in 1961 to simulate the growth of tumors. In addition to its biological applications, this model has relevance to many other types of stochastic growth phenomena with stable or marginally stable interfaces. When growing an Eden cluster one of the empty sites next to the aggregate (perimeter sites) is chosen randomly, and it is added to the cluster. A large cluster is obtained after having repeated this procedure many times. The particular method by which a site is selected for occupation is slightly different in the three basic variants A, B and C of the Eden model.

In the simulations of the most common version A, a single perimeter site is filled with probability $1/N_p$, where N_p is the total number of perimeter sites. Therefore, each nearest neighbour site to the cluster has the same probability to be occupied at the given time step. In version B one of the

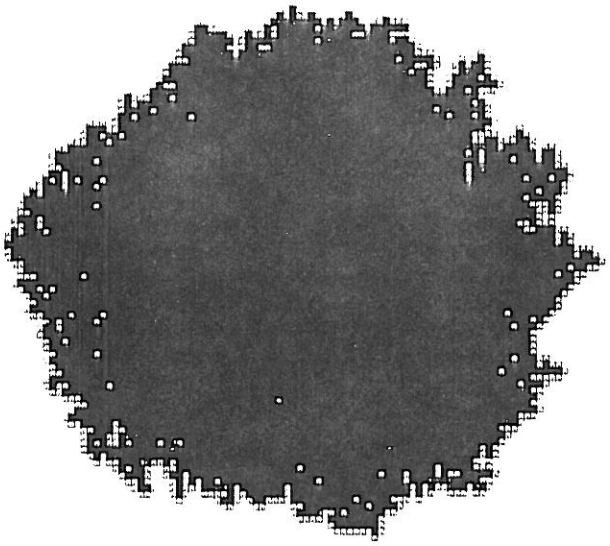

Figure 7.1. This Eden cluster consisting of 5000 particles was grown from a single seed by occupying randomly selected perimeter sites (version A).

free bonds is occupied by a particle with a probability $1/N_b$, where N_b is the number of bonds on the lattice connecting a filled and an empty site. In this way a perimeter site connected to the cluster through more than 1 bond has more chance to become occupied than in version A. Finally, it is possible to define a method in which all occupied surface sites of the cluster (sites with empty nearest neighbours) have the same probability to have a new neighbour in the next step. In this version i) a surface site is chosen with a probability $1/N_s$, where N_s is the number of surface sites. Then, ii) the new particle is added to one of the adjacent empty sites picked randomly. All three versions are expected to have the same scaling properties, but the rate of approaching the asymptotic behaviour can strongly depend on the particular variation used. In general, version C exhibits *faster convergence* than A and B (Jullien and Botet 1985).

Eden growth from a single seed leads to compact, d-dimensional objects which are nearly spherical and have a non-trivial surface (Fig. 7.1). The properties of the surface of a large Eden cluster can be investigated by determining $N_s(r, N)$, the number of perimeter or surface sites in a layer of width dr at a distance r from the origin. For a self-similar distribution of surface sites with a fractal dimension D one expects an expression of the form

(5.11) $N_s(r,N) \sim N^{\delta-1/D} f(r/N^{1/D})$, where δ is the exponent describing the increase of the total number of surface sites $N_S \sim N^\delta$ with N. According to the simulation and theoretical results (see e.g. Leyvraz 1985), for the Eden growth the exponent δ has a trivial value

$$\delta = d - 1. \tag{7.1}$$

In two dimensions $\delta = 1$, in complete agreement with our earlier statement about the global dimension of a self-affine surface.

Because of the self-affine nature of the surface, the above quoted expression (5.11) *does not hold* for the growth site distribution in Eden clusters. Numerical evidence shows that there is more than one relevant length scale determining the behaviour of $N_s(r,N)$ and, correspondingly, one has to use a more complex form for the scaling function $f(x)$ in (5.11) than for the self-similar case. In particular, the width $\sigma(N)$ of the distribution $N_s(r,N)$ was found to scale differently from its average radius $R(N)$ (Plischke and Ràcz 1985).

There are two factors determining the asymptotic behaviour of the surface site distribution of Eden clusters grown on a lattice with a single seed particle. In addition to the self-affine geometry of the surface zone, very large clusters become distorted because of the anisotropy of the underlying lattice. In order to see the weak *anisotropy* of the asymptotic overall *shape* of Eden clusters grown on a square lattice, aggregates containing of 5×10^7 particles have to be generated. For such sizes the deviation from a circular shape is about 2% (Freche *et al* 1985, Zabolitzky and Stauffer 1986).

There is a simple reason for the observed asphericity of single-seed Eden clusters. Imagine that one grows a cluster on a square lattice filling all perimeter sites simultaneously at each time step. It is easy to see that this procedure leads to a perfect diamond shape, since the distances of the layers perpendicular to the axes are larger by a factor $\sqrt{2}$ than the distances of layers perpendiclar to the diagonals. Correspondingly, the "velocity" of the interface depends on the local orientation of the surface. During random Eden growth this trivial anisotropy is not manifested in a direct way because

the local direction of the surface changes randomly. However, the interface always has parts with an average direction which results in differences in the growth velocity (Wolf 1987). In fact, it is possible to show analytically that Eden clusters grown on a hypercubic lattice in $d > 54$ dimensions must be anisotropic (Dhar 1985).

Instead of investigating the complex scaling of $N_s(r, N)$ it is more effective to concentrate on the properties of the *width of the surface region* $\sigma(N)$. Furthermore, as an alternative to the geometry corresponding to a single seed particle, Eden growth in a *strip geometry* can be studied to provide less biased data (Jullien and Botet 1985). This means that, for example, in two dimensions the seed is a line of L occupied sites and the growth is confined within a strip of width L using periodic boundary conditions. Simulation of the process in a $d-1$-dimensional "strip" has the advantage that the two parameters L and N controlling σ can be well separated.

Let us characterize the average height of an Eden deposit by

$$h \sim \bar{h} = \frac{1}{N_S} \sum_{i=1}^{N_S} h_i, \tag{7.2}$$

where $h = N/L$ is the average number of particles per column, N_S is the total number of surface sites and h_i is the distance of the ith surface site from the substrate. (7.2) expresses the fact that the vertical size grows linearly with the number of time steps (number of deposited particles), because of the compactness of the structure. In the single-seed case the number of particles N controls both the height, i.e., the mean radius $R \sim N^{1/d}$, and the "strip width" which corresponds to the circumference at the mean radius, $2\pi R \sim N^{1/d}$. Consequently, one expects that the scaling properties of the single-seed Eden clusters can be identified with those in strip geometry provided $h \sim \bar{h} \sim L \sim N^{1/d}$.

Let us define the surface width as

$$\sigma(L, h) = \left[\frac{1}{N_S} \sum_{i=1}^{N_S} (h_i - \bar{h})^2 \right]^{1/2}, \tag{7.3}$$

where $\bar{h}$ is given by (7.2). One expects that in the strip geometry there are two separate scaling regimes: i) for $h \ll L$ the fluctuations in the shape of the surface grow as some power of h, while ii) for $h \gg L$ the surface becomes stationary and its width depends on L algebraically. This behaviour can be described by the following scaling form (Vicsek and Family 1985, Jullien and Botet 1985)

$$\sigma(L,h) \sim L^{\alpha} f\left(\frac{h}{L^{z}}\right), \tag{7.4}$$

where the exponents α and z correspond to the stationary and "dynamic" scaling of the interface width, respectively. The scaling function $f(x)$ is such that

$$f(x) \sim \begin{cases} \sim x^{\beta} & \text{for } x \ll 1 \\ \simeq \text{constant} & \text{for } x \gg 1. \end{cases} \tag{7.5}$$

This is equivalent to

$$\sigma(L,h) \sim h^{\beta} \qquad \text{for} \qquad h/L^{z} \ll 1 \tag{7.6}$$

and

$$\sigma(L,h) \sim L^{\alpha} \qquad \text{for} \qquad h/L^{z} \gg 1. \tag{7.7}$$

Comparing (7.5) and (7.6) we find that

$$z = \alpha/\beta. \tag{7.8}$$

The scaling assumption (7.4) forms the basis of the investigations of Eden surfaces. Together with (7.7) it expresses the self-affine nature of the surface of Eden clusters, since in the $h/L^{z} \to \infty$ limit the size of the surface in the direction perpendicular to the substrate diverges as L^{α}, i.e., with a different exponent than its size L along the substrate. This is a situation analogous to the graph of the one-dimensional Brownian motion, where the

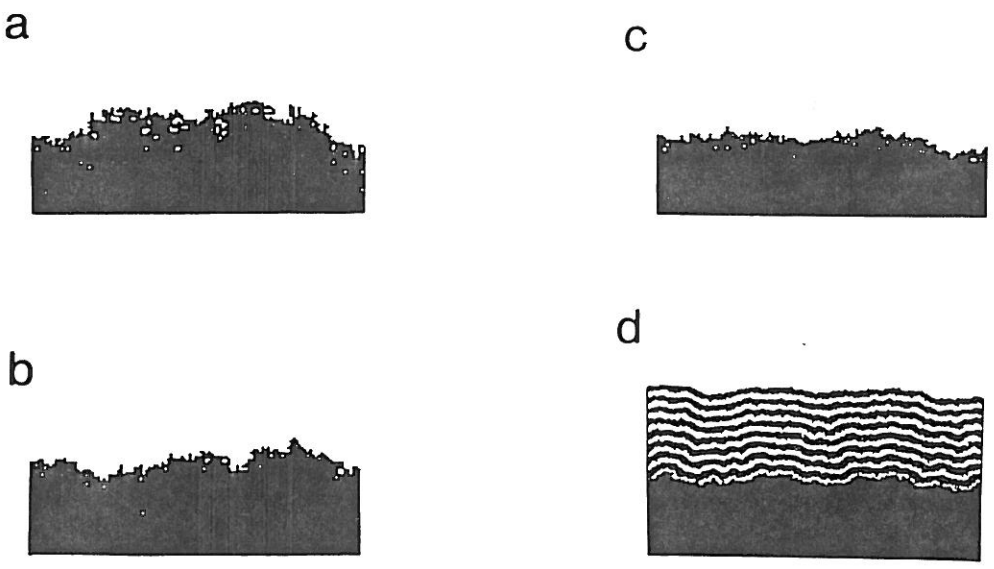

Figure 7.2. Eden deposits of 25000 particles generated on a substrate of width $L = 160$ using the noise reduction algorithm with $m = 1, 2, 4$ (a-c). Figure 7.2d shows the time evolution of a cluster for which at $N = 10000$ noise reduction with $m = 16$ was switched on (following a growth with $m = 1$) (Kertész and Wolf 1988)

distance of the particle at time t is plotted along the vertical axis versus the number of steps t (see Section 2.3.2.). For such a plot the average width of the curve (which is the square root of the mean squared displacement) scales as the square root of t representing the horizontal size of the sample.

Numerical investigation of the scaling properties of $\sigma(L, h)$ is surprisingly difficult. In order to see the precise asymptotic behaviour, an extremely large number of particles is needed because in the intermediate region the dependence of the effective exponent β is unusually complex as a function of the deposition height. The main reason for the slow convergence has its origin in the so called *intrinsic width* σ_i which is independent of L. According to this picture the surface width contains two additive terms: i) width coming from the relevant, long wavelength fluctuations, and ii) a size independent width σ_i which corresponds to the local stochastic configuration of the particles in a narrow zone at the surface. This means that for $h/L^z \to \infty$ one has $\sigma_\infty^2 = L^2 f_\infty^2 + \sigma_i^2$ (Kertész and Wolf 1988), and the second, correction to scaling term of the right-hand-side strongly affects the numerical results, especially in dimensions higher than 2. Here the quadratic summation arises

naturally if σ_∞ is regarded as the width of the convolution of two Gaussian distributions, one describing the long wavelength fluctuations and the other the intrinsic width.

The actual value of α and z has been investigated by a number of simulations. The situation for $d = 2$ seems to be settled: the numerical estimates are close to $\alpha = \frac{1}{2}$ and $z = \frac{3}{2}$. To observe scaling for $d = 3$ and $d = 4$ the noise-reduction method was applied which reduces the intrinsic width (Wolf and Kertész 1987a). During the application of this method to Eden growth, counters are placed on the perimeter sites and initially are set to have a value 0. Each time a perimeter site is selected for occupation, the counter is incremented by one, and the site is actually occupied only if the counter reaches a prescibed value m called noise-reduction parameter. As a result, "old" perimeter sites are occupied preferentially so that the holes, high steps and overhangs which are mainly responsible for the intrinsic width are suppressed (Fig. 7.2).

For a given noise-reduction parameter the surface width is expected to scale as (Kertész and Wolf 1988)

$$\sigma^2(L,h,m) = [a(m)L^\alpha f(h/L^z m^y)]^2 + \sigma_i^2(m), \tag{7.9}$$

where $a(m)$ is an m dependent constant. It is clear from the above relation that the exponents α and z are not affected by m and simulations with $m > 1$ can be used to estimate their values. The results are summarized below (Wolf and Kertész 1987b).

$$\begin{array}{lll} d = 2 & \beta = 0.33 \pm 0.015 & \alpha = 0.51 \pm 0.025 \\ d = 3 & \beta = 0.22 \pm 0.02 & \alpha = 0.33 \pm 0.01 \\ d = 4 & \beta = 0.15 \pm 0.015 & \alpha = 0.24 \pm 0.02. \end{array} \tag{7.10}$$

The above values are in good agreement with the scaling relationship $\alpha + z = \alpha + \alpha/\beta = 2$ following from theoretical arguments (Section 7.4). Furthermore, they suggest that $\alpha = 1/d$, in contradiction with theoretical results predicting either superuniversality ($\alpha = 1/2$ for all d) or $\alpha = 0$ for $d > 2$ (see Section

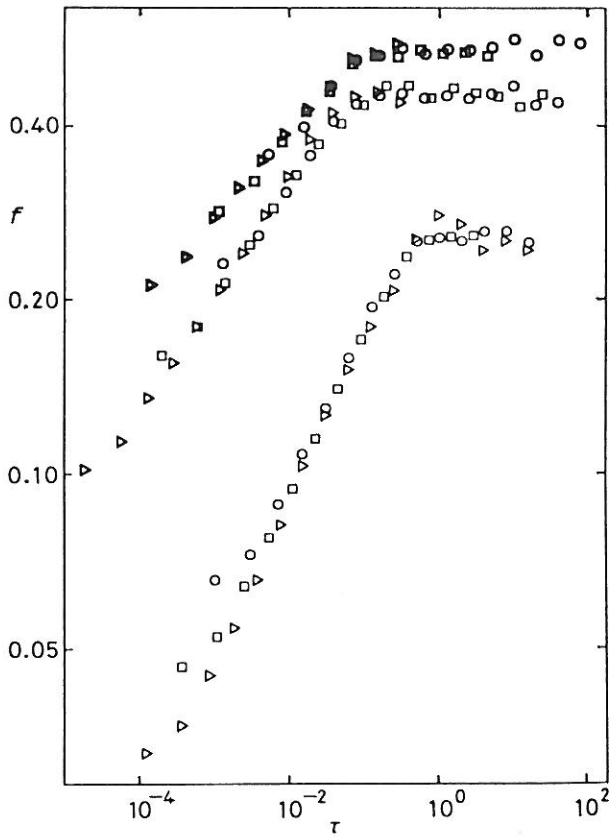

Figure 7.3. Scaling plot for $d = 2$ (lower curve, $L = 60$ (○), 120 (□), and 240 (▷)), for $d = 3$ (middle curve, $L_1 \times L_2 = 10 \times 10$ (○), 30×32 (□) and 120×128 (▷)), and for $d = 4$ (upper curve, $L_1 \times L_2 \times L_3 = 4 \times 4 \times 4$ (○), $9 \times 10 \times 10$ (□), and $30 \times 32 \times 32$ (▷)). The noise-reduction parameter is $m = 8$ for all data (Wolf and Kertész 1987b).

7.4). The best way to visualize the results of computer simulations is to plot the scaling function $f(x)$ using $\alpha = 1/d$ and $z = 2 - \alpha$. Fig. 7.3 shows a reasonable collapse of data for various values of L.

7.2. BALLISTIC AGGREGATION

In ballistic aggregation models the particles move along straight trajectories until they encounter the growing aggregate and stick to its surface irreversibly. This kind of kinetics is typical for experimental situations when molecules move in a low density vapour. Therefore, ballistic aggregation can be useful for the interpretation of technologically important processes, such

as vapour deposition on a cold substrate (Vold 1963, Sutherland 1966, Leamy *et al* 1980).

Two basic versions of the model have been considered recently. In the first case the particles move along randomly oriented straight lines, while trajectories are assumed to be parallel in the second type of models. In addition, the geometry of the substrate can also affect the results and, accordingly, ballistic aggregation on both a single seed (this Section) and surfaces (next Section) has been investigated.

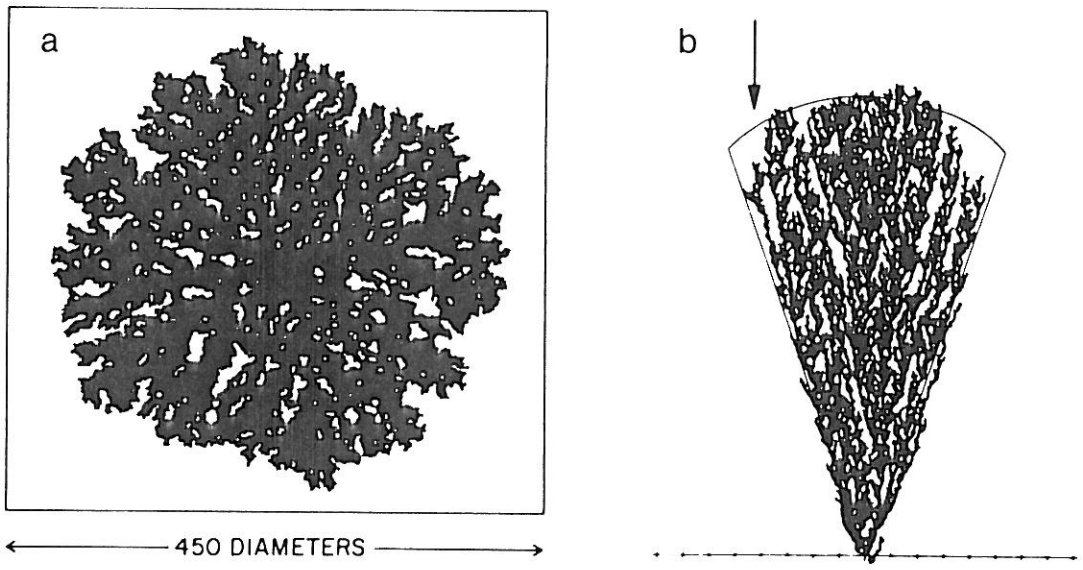

Figure 7.4. Off-lattice ballistic aggregates. (a) This cluster consisting of 180,000 particles was generated by simulating randomly oriented trajectories (Meakin 1985b). (b) Randomly positioned vertical trajectories lead to a fan-like structure when a single seed particle is used (Ramanlal and Sander 1985).

Fig. 7.4a shows a ballistic aggregate grown using a two-dimensional off-lattice model with a single seed particle and randomly oriented trajectories. In spite of the simplicity of the rules the structure of large ballistic aggregates is far from trivial. There are large, elongated holes and open streaks of various sizes in the cluster, however, the structure does not appear to be self-similar. Thus ballistic aggregates are not fractals. This statement can be made more quantitative by carrying out simulations (Meakin 1985,

Family and Vicsek 1985, Liang and Kadanoff 1985) and also follows from a simple theoretical argument (Ball and Witten 1984) given below.

For ballistic aggregates the considerations resulting in a causality bound for the fractal dimension of DLA clusters (See Section 6.1.1) take a considerably simpler form. In the case of straight trajectories and a fixed small density of the moving particles, the number of particles in the aggregate, $N(t)$, grows in time linearly with the cross-section of the cluster

$$\frac{dN(t)}{dt} \sim R(t)^{d-1}, \tag{7.11}$$

where $R(t)$ is the radius of the aggregate at time t. On the other hand,

$$\frac{dN(t)}{dt} = \frac{dN(t)}{dR(t)}\frac{dR(t)}{dt} \sim R^{D-1}v \tag{7.12}$$

Since v, the growth rate of the radius $R(t)$, can not increase indefinitely (in other words it must remain smaller than some v_{max}) we have

$$R^{d-D} \leq v_{max}, \tag{7.13}$$

therefore, $D = d$ has to be satisfied to guarantee $v_{max} < \infty$ when $R(t) \to \infty$ ($D > d$ is excluded for obvious reasons).

Although the dimension of ballistic aggregates turns out to be the same as the Euclidian dimension of the space they are grown in, they exhibit non-trivial scaling behaviour. Consider the following version of the model. A seed particle is put into the origin of a square lattice and the rest of the particles move parallel to the y axis with random x coordinates till they either disappear or stick to the growing cluster (the latter takes place if a particle arrives at a site adjacent to the aggregate). The resulting cluster looks like a *fan* with higher density in the central region and long holes near its edge. This process can be formulated easily for the off-lattice case as well, leading to a similar structure (Fig. 7.4b).

The scaling behaviour of the *density distribution* $\rho(r, \theta)$ within the fan

can be described as a function of the distance from the seed, r, and the angle θ measured from the y direction. Here the density is defined as the number of particles within the area $r\Delta r\Delta\theta$. According to the simulations $\rho(r,\theta)$ can be well represented by the scaling form (Liang and Kadanoff 1985)

$$\rho(r,\theta) \sim r^{-\mu} f\left(r^{\vartheta}(\theta - \theta_c)\right), \tag{7.14}$$

where the scaling function $f(x) \simeq$ constant for $x \ll 1$ and $f(x) \ll 1$ for $x \gg 1$, θ_c is a critical angle corresponding to the region close to the edges of the fan, $\theta > \theta_c$, and μ and ϑ are scaling indices. This assumption is supported by the fact that the data points for ρr^{μ} as a function of the renormalized angle $r^{\vartheta}(\theta - \theta_c)$ fall onto the same universal curve for various r and θ. In the case of off-lattice aggregates the best collapse is obtained using $\theta_c = (15.5 \pm 0.7)°$, $\mu = 0.13 \pm 0.05$ and $\vartheta = 0.39 \pm 0.05$ (Joag *et al* 1987). These values for the exponents agree within the error limits with those obtained for the on-lattice case. The critical angle, however, is considerably less than $\theta_c \simeq 32°$ found in the simulations carried out on the square lattice.

Let us now investigate the average density in the region $|\theta| < \theta_c$ as a function of r. For a fixed such angle the density within a large aggregate approaches a constant as $r \to \infty$. This means that the fan has a trivial dimension $D = d$ as was mentioned before. On the other hand, the approach to the constant density is very slow, and follows a power law of the form (Liang and Kadanoff 1985)

$$\rho(r) = \rho_\infty + Ar^{-\beta}, \tag{7.15}$$

where ρ_∞ and A are constants and β is a non-trivial correction to the dimensionality. The above relation is analogous to the expression (2.37), assuming that $l \sim 1/r$. Therefore, (7.15) can be regarded as an indication of the *fat fractal* character of ballistic aggregates. The exponent β was determined from the slopes of the plots $\ln(\rho - \rho_\infty)$ versus $\ln r$ for both the off-lattice and the square lattice cases giving respectively $\beta \simeq 0.55$ and $\beta \simeq 0.66$. Thus the metadimension β appears to be non-universal.

7.3. BALLISTIC DEPOSITION

In this section, ballistic aggregation of particles onto surfaces will be discussed. We assume that the particles are released from randomly chosen launching points and move along parallel straight lines till they are attached to the aggregate. In general, the *angle of incidence* ϑ (the angle between the trajectories and the normal vector to the surface) can be varied from 0 (vertical trajectories) to $\pi/2$. This situation is common in a number of technologies used to control electrical, optical and other physical properties of surfaces by means of vapour deposition.

In an actual simulation of ballistic deposition the *strip geometry* with periodic boundary conditions is used. The linear size of the substrate is denoted by L. The particles are launched at randomly selected positions at a height of $h_{max} + 1$ which is the maximum height of any particle in the deposit. Then the particles follow a straight trajectory with a prescribed angle of incidence until they contact either a particle in the deposit or reach the original surface. At the point of the first contact they are stopped and become part of the growing deposit. In the lattice version of the model with $\vartheta = 0$ it is easy to see that there is only one active perimeter site (a site which has the possibility to be filled in the next step) in each column. Since one needs to record only the height of these L sites such an algorithm is fast and does not require much computer time. The off-lattice case with $\vartheta \neq 0$ can be simulated effectively by choosing a suitable underlying lattice to find particles near the trajectory of a moving particle.

Both the experiments and computer simulations showed that in the case of non-zero incidence angle, *columnar structures* grow on the surface. This columnar morphology is most distinctive for large ϑ, and the angle ς between the growth direction of the columns and the normal to the surface is less than the angle of incidence. Investigations of vapour and sputter-deposited aluminium and rare-earth-metal thin films suggested the *empirical relationship* (Nieuwenheuzen and Hannstra 1966, Leamy *et al* 1980)

$$\tan\varsigma \simeq \frac{1}{2}\tan\vartheta \tag{7.16}$$

known as the "tangent rule". It is easy to see why ζ should be less than ϑ: Particles passing the "high" side of an existing column can be caught and cause the column to tilt towards the normal. However, (7.16) has not been shown to hold by any rigorous theoretical argument.

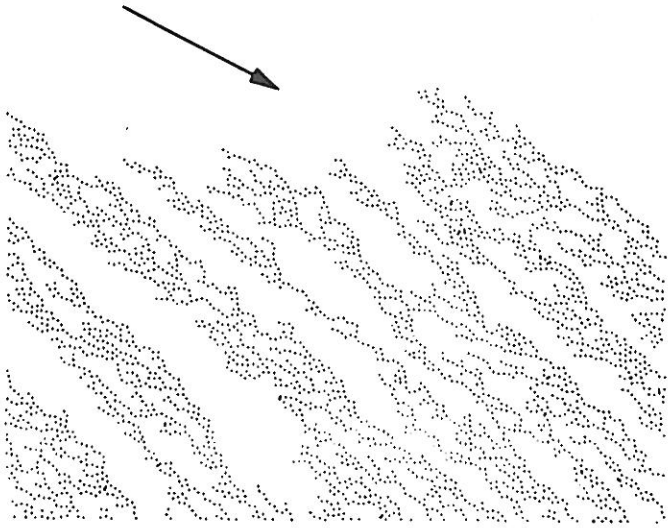

Figure 7.5. Off-lattice ballistic deposit obtained for a fixed angle of incidence $\vartheta = 60°$ (Ramanlal and Sander 1985).

Fig. 7.5 shows a typical configuration obtained in a relatively small scale simulation of two-dimensional off-lattice ballistic deposition with a fixed angle of incidence $\vartheta = 60°$. The deposit has a columnar structure and the deviation of the direction of growth from the direction of the incident beam is qualitatively consistent with the tangent rule. To check whether the tangent rule is qualitatively valid for ballistic deposition one needs a quantitative determination of the growth direction ζ. This can be achieved by noting that for off-lattice aggreggates the incoming particles make contact with only a single particle belonging to the deposit. Thus the deposit can be considered as a set of trees which consist of particles connected to the same root particle at the surface. For large ϑ these trees can be identified with the columns. The growth direction of a tree is given by the expression (Meakin et al 1986b)

Table 7.1. Dependence of some characteristic quantities on the angle of incidence ϑ obtained from simulations of two-dimensional off-lattice deposition. ς – mean angle of tree growth, ς' – prediction of the tangent rule, and $\vartheta - \varsigma$ – a quantity which appears to saturate close to 16° for large angles of incidence. All angles are shown in degrees (Meakin *et al* 1986b).

ϑ	ς	ς'	$\vartheta - \varsigma$
10	11.55	5.04	-1.55
20	16.17	10.31	3.83
30	23.94	16.10	6.06
40	31.02	22.76	8.98
50	39.46	30.79	10.54
60	47.13	40.89	12.87
70	55.46	53.95	14.54
80	63.93	70.57	16.07

$$\tan\varsigma(j) \simeq \frac{\sum_{i=n_j}^{n_j+\Delta n_j} x_i - x_{j0}}{\sum_{i=n_j}^{n_j+\Delta n_j} y_j}, \tag{7.17}$$

where x_i and y_i are respectively the horizontal and vertical coordinates of the ith particle in the jth tree, x_{j0} and $y_{j0} = 0$ are the positions of the root particles and the summation is taken over Δn_j particles added to the tree already consisting of $n_j \gg 1$ particles. The average growth direction can be obtained by averaging over the angles corresponding to the individual trees.

The results of simulations for the ϑ dependence of ς, and $\varsigma' = \tan^{-1}(\frac{1}{2}\tan\vartheta)$ (which is the prediction of the tangent rule) are displayed in Table 7.1. This table demonstrates that the deviations from the tangent rule are quite strong. It is evident from this table that the simplest two-dimensional ballistic aggregation models can not be used to explain the tangent rule on a quantitative basis.

Let us now consider the structure of the surface of deposits generated

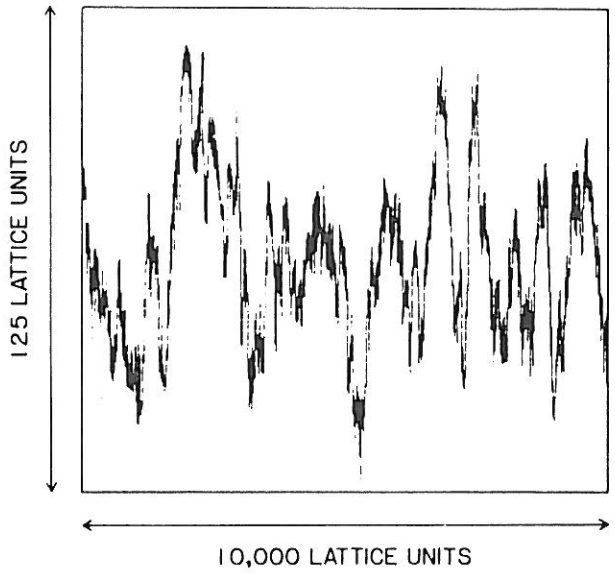

Figure 7.6. Section from the surface of a deposit grown on the square lattice to an average height of 5000 lattice units along a base line of length 2^{18} units (Meakin *et al* 1986b).

on a square lattice with $\vartheta = 0$. Fig. 7.6 shows part of the surface of a large deposit. The apparent similarity of this plot to Fig. 2.13 exhibiting the graph of the one-dimensional Brownian motion indicates the self-affine nature of the surface. This analogy can be made more quantitative by studying the variance of the heights of the active perimeter sites. According to the simulations to be discussed later, in analogy with the Eden model in a strip geometry, the width of the surface defined by (7.3) scales as $\sigma(L,h) \sim h^{\beta}$ for $h \ll L$ (7.6) and $\sigma(L,h) \sim L^{\alpha}$ if $h \gg L$ (7.7) (Family and Vicsek 1985).

The scaling of σ as a function of L for $h \gg L$ indicates the *self-affine* nature of the surface of ballistic deposits. In Section 2.3.2. it was discussed that if the root mean square distance of a one dimensional random motion scales with the number of steps t as $\langle X^2(t)\rangle^{1/2} \sim t^H$, then the graph of the actual distance of the walker from the origin as a function of t is a self-affine function with a local fractal dimension $D = 2 - H$. Furthermore, $X(t)$ has the self-affine property $X(t) \sim b^{-H} X(bt)$, where b is a rescaling factor and H is a characteristic exponent. In the present case, for $d = 2$ the role of t is played by the actual distance x along the substrate, and $X(t)$ corresponds to $\tilde{h}(x) = h(x) - \bar{h}$, where $h(x)$ is the height of the active perimeter site in column x (there is only one such site in each column). Therefore, in the

$h \to \infty$ limit the surface of the deposits satisfies

$$\tilde{h}(x, \bar{h} \to \infty) \sim L^{-\alpha} \tilde{h}(Lx, \bar{h} \to \infty). \tag{7.18}$$

To incorporate the $\sigma \sim h^{\beta}$ behaviour for $h \ll L$ one assumes that (Meakin *et al* 1986b)

$$\tilde{h}(x, \bar{h}) \sim \bar{h}^{\beta} f(x/\bar{h}^{1/z}), \tag{7.19}$$

where the scaling function $f(y)$ is assumed to be a randomly changing function with $|f(y)| < Const$ for $y \gg 1$, and

$$f(y) \sim L^{-\alpha} f(Ly) \qquad \text{for} \qquad y \ll 1. \tag{7.20}$$

The latter condition is needed to satisfy (7.18). Since the width of a self-affine function defined by (7.19) scales as y^{α}, we see that $\sigma \sim L^{\alpha}$ for $h \ll L$ is also satisfied if $\alpha/z = \beta$. Expressions analogous to (7.18) and (7.19) are expected to be valid in dimensions higher than 2 as well both for ballistic deposits and Eden clusters generated in the strip geometry.

One consequence of (7.18) is that the intersection of the surface and a plane placed at a distance $\bar{h}$ from the substrate has the fractal dimension

$$D = d - 1 - \alpha. \tag{7.21}$$

To see this we recall rule f) of Section 2.2. relating the fractal dimension of the intersection of two fractals of dimensions D_A and D_B through the expression $D_{\cap} = D_A + D_B - d$. For a self-affine deposit the local fractal dimension is $D_A = d - \alpha$ (see Section 2.3.2., where D_{local} was shown to be equal to $2 - \alpha$ for $d = 2$) and the dimension of the plane parallel to the substrate is $D_B = d - 1$. Although the deposits do not have a well defined local fractal dimension because of the coincidence of the crossover scale and the lattice spacing (this question was discussed at the beginning of this Chapter), the global behaviour of the cross-section is not affected by

the crossover scale and (7.21) is expected to hold.

The *scaling of the surface width* has been extensively studied for a number of deposition models. In the case of the square lattice large scale simulations (Meakin *et al* 1986b) led to numerical values for the exponents α, β and z close to the theoretical prediction (Kardar *et al* 1986)

$$\alpha = 1/2, \qquad \beta = 1/3 \quad \text{and} \quad z = 3/2. \tag{7.22}$$

The surface width can also be determined for off-lattice ballistic deposits as a function of the angle of inclination ϑ. For off-lattice aggregates the surface sites are not well defined and the surface thickness should be calculated from a modified expression (Meakin and Jullien 1987)

$$\sigma(L,h) = \frac{1}{N} \sum_{i=M}^{M+N} |h_i - h_{i+1}|, \tag{7.23}$$

where h_i is the minimum distance from the substrate of the point at which the ith particle is deposited and $N - M$ is the increment in the deposit mass over which the characteristic quantities are determined. According to the $2d$ simulations the L dependence of $\sigma(L,h)$ is described by the exponent $\alpha = 1/2$, for all ϑ. The exponent β, however, was found to depend on the angle of inclination. This is demonstrated by the following few selected values: $\beta \simeq 0.343$ ($\vartheta = 0$), $\beta \simeq 0.281$ ($\vartheta = 45°$) and $\beta \simeq 0.402$ ($\vartheta = 80°$).

In addition to the ϑ dependence of β, its value is changed when the deposition process is modified to take into account *surface restructuring.* Consider a lattice model with angle of inclination equal to zero, in which a particle after having contacted the deposit is moved to a new surface site with the smallest height within a given region surrounding the point of first contact. Such and analogous relaxation rules tend to smooth out irregularities and result in estimates of β close to 1/4 (Family 1986, Meakin and Jullien 1987).

Large scale simulations of ballistic deposition in three dimensions seem to support the scaling assumption (7.4) for the width of the surface. The

numerical results $\alpha \simeq 0.33$ and $\beta \simeq 0.24$ obtained for the corresponding exponents (Meakin *et al* 1986b) suggest that the exact value of α in $d = 3$ might be equal to $1/3 = 1/d$. In addition, $\beta = 1/4$ is consistent with the scaling relation $\alpha + \alpha/\beta = 2$. The situation seems to be similar to that of Eden growth: there is only one independent exponent describing the scaling of the surface width and it is found to be close to $\alpha = 1/d$ (Wolf and Kertész 1988). While the situation is settled for the two-dimensional case, the theoretical predictions for higher dimensions are not consistent with the above numerical results. It is not clear whether there exists an upper critical dimension for the problem of growing self-affine surfaces above which $\alpha = 0$.

7.4. THEORETICAL RESULTS

The theoretical treatment of growing self-affine interfaces is based on constructing a continuum differential equation for describing the motion of the interface. We shall consider first the general case of a random interface evolving in the strip geometry with a $d-1$ dimensional substrate of linear size L. Since the exponents α and β characterizing the width of the interface σ were found to be less than unity, both σ/L and σ/h go to zero as $\sigma \to \infty$. It is convenient to ignore overhangs so that h can be considered as a single valued function of $\vec{x}$. Therefore, one can assume that local coarse scale derivatives dh/dx exist. Let us now express the velocity of the interface $h(\vec{x},t)$ as a function of its local gradient. To take into account the stochastic nature of the growth one writes down the simplest non-linear Langevin equation for $\tilde{h} = h - \bar{h}$ (comoving frame) in the form (Kardar *et al* 1986)

$$\partial\tilde{h}(\vec{x},t)/\partial t = \gamma\nabla^2\tilde{h}(\vec{x},t) + \lambda[\nabla\tilde{h}(\vec{x},t)]^2 + \eta(\vec{x},t), \qquad (7.24)$$

where the time variable t is associated with the average deposition height $\bar{h}$. In the above equation the first term describes the relaxation of the interface due to the surface tension γ. Its meaning is quite obvious; protrusions (places with local curvature $\nabla^2\tilde{h}$ less than zero) tend to disappear under the influence of the smoothing effect of surface tension. Such effects are expected to be particularly important if *surface restructuring* is allowed.

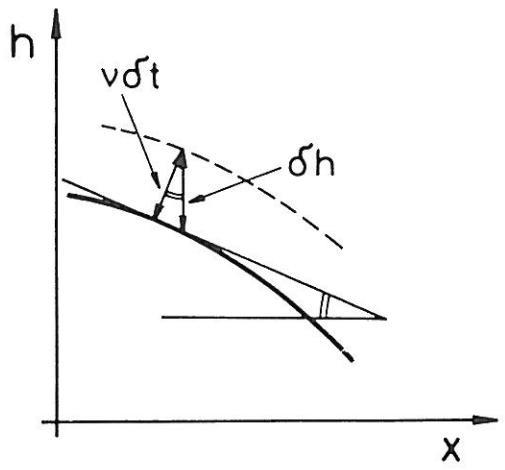

Figure 7.7. Schematic picture showing the increment of h as the growth locally occurs along the normal to the interface.

The second term in (7.24) is the lowest-order non-vanishing term in a gradient expansion. Its inclusion can be justified by the following argument. Consider, for example, the growth of an Eden cluster in two dimensions. In general, the growth takes place in a direction locally normal to the interface. When a particle is added, the increment projected onto the h axis is $\delta h = [(v\delta t)^2 + (v\delta t \nabla h)^2]^{1/2}$ (Fig. 7.7) which leads in the weak gradient limit to

$$\partial h/\partial t = v[1 + (\nabla h)^2]^{1/2} \simeq v + (v/2)(\nabla h)^2 + ..., \qquad (7.25)$$

where v is the velocity normal to the interface. The above expression reduces to the second term in (7.25) after transformation to the comoving frame and is supposed to play a relevant role in situations where *lateral growth* is allowed.

The third term in expression (7.24) is included to take into account the fluctuations. The noise denoted by $\eta(\vec{x}, t)$ is assumed to have a Gaussian distribution, so that $\langle \eta(\vec{x}, t) \rangle = 0$, and

$$\langle \eta(\vec{x}, t)\eta(\vec{x}', t') \rangle = 2C\delta^d(\vec{x} - \vec{x}')\delta(t - t'). \qquad (7.26)$$

Let us use Eq. (7.24) to obtain a scaling relation among the exponents α, β and z in addition to (7.8). For this purpose we assume that for large scale solutions one can neglect the noise in (7.24). Furthermore, if the surface

tension effects are small, we can omit the first term in (7.24) as well. Then we have the following simplified equation

$$\partial\tilde{h}/\partial t \simeq (\nabla\tilde{h})^2 \tag{7.27}$$

which has a solution of the form (7.19) with $\bar{h} \sim t$. This can be checked by inserting (7.19) into (7.27) (Meakin *et al* 1986b). When carrying out this substitution it is easy to see by comparing the leading terms in t that the two sides of Eq. (7.27) are equal if

$$z + \beta z = z + \alpha = 2 \tag{7.28}$$

(where (7.8) $z = \alpha/\beta$ was used), and $f(\vec{y})$ satisfies

$$\beta f(\vec{y}) - \frac{1}{z}\vec{y}\frac{\partial}{\partial y} f(\vec{y}) = \left[\frac{\partial}{\partial y} f(\vec{y})\right]^2 . \tag{7.29}$$

It can be shown by similar arguments that the scaling relation (7.28) is not affected if the surface tension term is also included into the calculations. In addition to the above heuristic arguments, more complete proofs of (7.28) can be given by application of mode coupling techniques to the full Eq. (7.24) (Krug 1987) or by mapping it to the directed polymer problem in a $(d+1)$-dimensional space (Kardar and Zhang 1987).

In order to determine the actual values of the exponents in (7.28) the formalism of the dynamic renormalization group can be applied to the full stochastic problem defined by Eq. (7.24) (Kardar *et al* 1986). The corresponding method was elaborated for the Burgers's equation which can be obtained from (7.24) using the transformation $\vec{v} = -\nabla\tilde{h}$. Instead of reproducing the calculations, here we discuss the results which can be summarized as follows. Eq. (7.24) embodies three different universality classes, depending on the values of the parameters γ and λ.

i) The $\gamma = \lambda = 0$ case corresponds to random deposition of particles with no surface restructuring or sticking of the particles to each other. Then for $L \gg 1$ the columns grow according to the Poisson statistics describing the

probability that the number of particles in a given column is equal to h if $\bar{h}$ particles per column have been deposited. Thus $\sigma \sim \bar{h}^{1/2}$ is given by the central limit theorem, and

$$\beta = 1/2. \tag{7.30}$$

Since the size of the substrate does not have an effect on σ, the other two exponents can be regarded to be equal to zero.
ii) If $\lambda = 0$, the evolution of the interface is dominated by surface restructuring. For this case

$$\alpha = (3-d)/2, \qquad \beta = (3-d)/4 \qquad \text{and} \qquad z = 2 \tag{7.31}$$

can be obtained by Fourier transforming (7.24) (Edwards and Wilkinson 1982).
iii) The third universality class corresponds to the general case when neither γ nor λ is equal to zero. From the dynamical renormalization group approach the following exponents were found

$$\alpha = (3-d)/2, \qquad \beta = (3-d)/3 \qquad \text{and} \quad z = 3/2. \tag{7.32}$$

It is clear from (7.31) and (7.32) that the critical dimension appearing in these theories is $d = 3$, where logarithmic corrections are expected to complicate the situation.

A comparison of the above results with those obtained in the simulations leads to satisfactory agreement between the theory and numerical experiments in two dimensions. Indeed, for $d = 2$ both the Eden growth and ballistic deposition results suggest $\alpha = 1/2$ and $\beta = 1/3$ in accord with (7.32). Simulations of ballistic aggregation with surface restructuring resulted in estimates for β close to $1/4$ which is predicted by (7.31).

The situation is more controversial in higher dimensions. The simulations with no restructuring provide numerical evidence for the conjecture that $\alpha = 1/d$ and the validity of the scaling relation $\alpha + z = 2$ which allows

one to obtain the rest of the exponents once α is known. These results are in disagreement with the theoretical predictions. It is apparent from (7.32) that the perturbative dynamic renormalization method suggests an upper critical dimension equal to $d = 3$. According to very recent theoretical arguments $d_c = 3$ corresponds to the weak coupling regime (i.e., to small noise), and for large $\langle \eta(\vec{x}, t)^2 \rangle$ another regime exists with a dimension independent (or superuniversal) exponent $z = 1.5$ (Kardar and Zhang 1987, McKane and Moore 1988).

As concerning ballistic deposition with surface restructuring three-dimensional simulations of the off-lattice process (Jullien and Meakin 1987) indicate that the surface width diverges logarithmically with $\bar{h}$ and L in a better agreement with the theoretical result $d_c = 3$ (7.31) obtained for this case.

Let us now concentrate on the development of a *mean-field approach* to the description of the *columnar geometry* of ballistic aggregates (Ramanlal and Sander 1985). This continuum theory which is to treat aggregation with uniaxial trajectories is based on the tangent rule (7.16) relating the angle of incidence ϑ to the angle of holes or columns ς, where both angles are measured with respect to the normal to the envelope of the surface. It is easy to understand why $\vartheta > \varsigma$: the particles arrive at the surface of the columns close to their most advanced parts and this results in a growth closer to the normal. Although (7.16) does not hold precisely, this fact does not change the general features of the theory.

The tangent rule can be used as a local prescription for the motion of the interface. According to this assumption each element of the surface moves in the direction which is determined by (7.16). For the envelope of the fan structure of Fig. 7.4b the interface in the long time limit satisfies (Ramanlal and Sander 1985)

$$\begin{aligned} \frac{\partial y}{\partial x} &= -\tan\vartheta, \\ \frac{y}{x} &= \tan(\theta), \end{aligned} \tag{7.33}$$

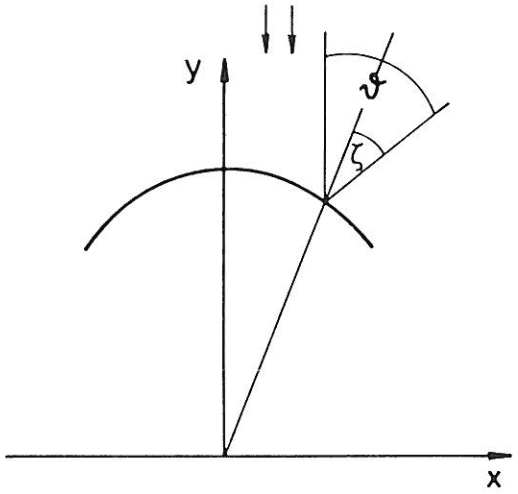

Figure 7.8. Schematic picture of the envelope of the interface (used to construct Eqs. 7.33).

where θ is measured from the y axis (Fig. 7.8). On the other hand, we must have $\theta = \vartheta - \varsigma$, since the surface moves along a straight line originating at the seed (because of the tangent rule). The solution of the set of equations (7.16) and (7.33) can be obtained by converting to polar coordinates. Then $\partial r/\partial\theta = r\tan\varsigma$ with the polar angle

$$\theta = \tan^{-1}[\tan\vartheta/(2+\tan^2\vartheta)] \tag{7.34}$$

follows from the tangent rule. The solution is

$$\begin{aligned} r &= r_0 f(\theta), \\ f(\theta) &= \frac{1}{\sqrt{2}|\sin\theta|}\frac{(n+1)^{1/4}(n-1)^{1/2}}{(3n-1)^{3/4}}, \\ n &= (1-8\tan^2\theta)^{-1/2}, \end{aligned} \tag{7.35}$$

where r_0 is a time dependent constant. $f(\theta)$ can laso be written in a more compact form

$$f(\theta) = (\cos\vartheta)^{1/2}/\cos\varsigma. \tag{7.36}$$

The most important feature of the solution appears quite naturally in (7.35).

When $\tan\theta = 1/\sqrt{8}$, n diverges. This condition corresponds to an angle $\theta \simeq 19.5°$ which is in good agreement with the simulation results. One way to understand this result is to note that (7.34) has a maximum at 19.5°, thus one never expects to see a fan with an opening angle away from the incident direction larger than this value. However, the above angle is not universal since in the case of the square lattice, (discussed in Section 7.2.), the opening angle was found to be about 32°.

Eq. (7.36) describes the static behaviour of the surface. In order to determine the actual motion of the interface one writes for the velocity of a point of the interface whose normal is $\hat{\mathrm{n}}$

$$\vec{\mathrm{v}} = v\hat{\mathrm{m}} = -(\hat{\mathrm{n}} \cdot \vec{\mathrm{J}}/\rho)\hat{\mathrm{m}} = v_0 f, \tag{7.37}$$

where $\hat{\mathrm{m}}$ is a unit vector in a direction between the incident beam and the normal, as given by the tangent rule, $\vec{\mathrm{J}}$ is the constant flux of incoming particles per unit area per unit time, and ρ is the local density. In the above expression f is given by (7.36) in order to be consistent with the solution obtained before for a fixed r_0. Eq. (7.37) has to be completed by the condition that there is no growth if $\cos\vartheta < 0$ (the surface is in a geometrical shadow). Finally, the velocity of the interface in a given direction $\hat{\mathrm{k}}$ can be expressed as

$$v_k = \frac{\hat{\mathrm{n}} \cdot \vec{\mathrm{v}}}{\hat{\mathrm{n}} \cdot \hat{\mathrm{k}}}. \tag{7.38}$$

Returning to polar coordinates with $\hat{\mathrm{k}} = \hat{\mathrm{r}}$, Eqs. (7.37) and (7.38) can be written in the form

$$\begin{aligned} \partial r(\theta,t)/\partial t &= v_0[(1+Q^2)\cos\vartheta]^{1/2}, \\ Q &= \partial r/\partial\phi, \\ \cos\vartheta &= (\cos\theta - Q\sin\theta)/(1+Q^2)^{1/2}. \end{aligned} \tag{7.39}$$

It can be checked by direct insertion of (7.35) into (7.39) that the former is an exact solution to the partial differential equation (7.39), with the initial

condition of growth from a point. For other initial conditions (7.39) can be treated by either stability analysis or numerical integration.

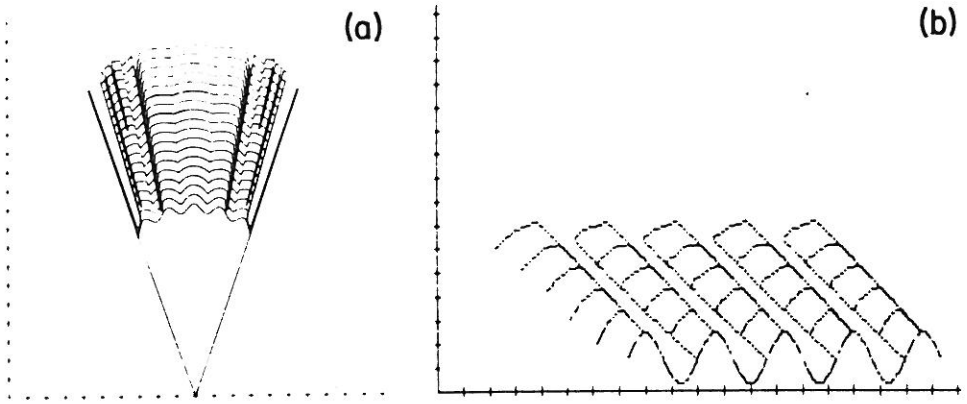

Figure 7.9. Numerical solutions of Eq. (7.39) for perturbed initial conditions. (a) Growth on a seed particle, and (b) on a line (Ramanlal and Sander 1985).

The actual solution depends on the roughness of the initial conditions. It can be shown that the asymptotic solution (7.39) is *marginally stable*, therefore, a smooth enough initial interface does not lead to instabilities. Let us assume that initially the surface looks like (Ramanlal and Sander 1985)

$$\delta(\theta, 0) = \delta_0 \cos(m\theta) \tag{7.40}$$

representing the fluctuations in the profile due to the random distribution of incoming particles. If $\delta_0 \ll 1$, the surface remains smooth because of the marginal stability of the solutions of (7.39). However, if (for example) $\delta_0/\bar{r}(0) = 0.05$ and m=44, the long empty strips characteristic for the fan structure appear, as is demonstrated in Fig. 7.9a. The streaks and ragged edges of Fig. 7.4b probably arise in this way. This suggests that the specific shape of ballistic aggregates emerges from the interplay of fluctuations (rough initial condition) and the consequent geometrical shadowing. The same line of reasoning and a periodic initial condition give rise to the growth of columns shown in Fig. 7.9b.

The main conclusion of the above mean-field continuum theory for

ballistic deposition is the following. The columns are nucleated due to the random nature of the deposition. Whenever the height per width of a cluster is large enough to produce geometrical shadow, this non-linear effect gives rise to the growth of a distinct column growing out from the given seed cluster.